DEPARTMENT OF THE NAVY

DAVID TAYLOR MODEL BASIN

HYDROMECHANICS

AERODYNAMICS

STRUCTURAL MECHANICS

APPLIED MATHEMATICS

A METHOD FOR ELIMINATING THE EFFECT OF END CONDITIONS ON THE STRENGTH OF STIFFENED CYLINDRICAL SHELLS

by

Robert F. Keefe and Robert D. Short, Jr.

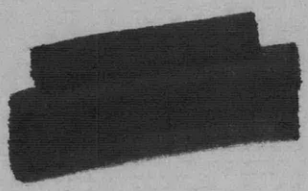

STRUCTURAL MECHANICS LABORATORY

RESEARCH AND DEVELOPMENT REPORT

September 1961

Report 1513

PRNC-TMB-648 (Rev. 3-58)

DEPARTMENT OF THE NAVY
DAVID TAYLOR MODEL BASIN
WASHINGTON 7, D.C.

IN REPLY REFER TO
9110/Subs
5606 5
(725:MEL:lkg)
Ser 7-392
13 October 1961

From: Commanding Officer and Director, David Taylor Model Basin
To: Chief, Bureau of Ships (442) (in duplicate)

Subj: Strength of stiffened cylindrical shells; a method of eliminating effects of end conditions on

Encl: (1) DATMOBAS Report 1513 entitled "A Method for Eliminating the Effect of End Conditions on the Strength of Stiffened Cylindrical Shells"
2 copies

1. In enclosure (1) a method of eliminating the weakening influences of bulkheads is presented whereby the thickness of plating and the length of the thickened plating away from the bulkheads could be adjusted. Enclosure (1) also presents test results validating the method. The test results indicate that failure could be shifted away from the ends of the cylinder and the collapse pressure could be increased by 4 percent over that of another cylinder in which the plating at the bulkheads was not thickened and the first bay length was 2/3 the length of the others.

E. E. Johnson

E.E. JOHNSON
By direction

Copy to:
BUSHIPS (106), with 1 copy of encl (1)
(320), with 1 copy of encl (1)
(335), with 3 copies of encl (1)
(420), with 1 copy of encl (1)
(421), with 1 copy of encl (1)
(423), with 1 copy of encl (1)
(440), with 1 copy of encl (1)
(443), with 1 copy of encl (1)
(525), with 2 copies of encl (1)
(633), with 1 copy of encl (1)

9110/Subs
560
(725:MEL:lkg)
Ser 7-392
13 October 1961

Copy to:
CHONR (439), with 1 copy of encl (1)
(466), with 1 copy of encl (1)
CNO (Op 311), with 1 copy of encl (1)
CDR, USNOL, with 1 copy of encl (1)
DIR, USNRL (Attn: TID), with 1 copy of encl (1)
NAVSHIPYD PTSMH, with 2 copies of encl (1)
NAVSHIPYD MARE, with 2 copies of encl (1)
NAVSHIPYD CHASN, with 2 copies of encl (1)
CDR, ASTIA, with 10 copies of encl (1)
SUPSHIP, Groton, with 1 copy of encl (1)
EB Div, Gen Dyn Corp, with 1 copy of encl (1)
SUPSHIP, NNS, with 1 copy of encl (1)
NNS SB and DD Co, with 1 copy of encl (1)
SUPSHIP, Pascagoula, with 1 copy of encl (1)
Ingalls SB Corp, with 1 copy of encl (1)
SUPSHIP, Camden, with 1 copy of encl (1)
New York SB Corp, with 1 copy of encl (1)
Dir of Def R and E, Attn: Tech Lib, with 1 copy of encl (1)
CO, USNROTC and NAVADMINU MIT, with 1 copy of encl (1)
O in C, PGSCOL, Webb, with 1 copy of encl (1)

DTMB (140)
(705)
CF

A METHOD FOR ELIMINATING THE EFFECT OF END CONDITIONS ON THE STRENGTH OF STIFFENED CYLINDRICAL SHELLS

by

Robert F. Keefe and Robert D. Short, Jr.

September 1961

Report 1513
S-F013 03 02

TABLE OF CONTENTS

LIST OF FIGURES

LIST OF TABLES

ABSTRACT

A pair of stiffened cylinders was subjected to external hydrostatic pressure to establish the adequacy of a design procedure for eliminating the effect of end conditions on strength. The cylinders were machined from a thick tube and were identical to those described in TMB Report 1326 except for the size and spacing of the frames and the thickness of the shell at the ends. The cylinders failed by axisymmetric shell yielding in the second full-length bay at identical collapse pressures. Test results indicated that, with these end conditions, the collapse pressure could be increased by 4 percent over that for a similar model in which the first bay length was two thirds of the length of the others, and failure could be shifted away from the ends of the cylinder.

INTRODUCTION

In experiments with stiffened cylindrical shells, failures in the axisymmetric yield mode have usually occurred in bays adjacent to holding bulkheads at lower pressures than those calculated from analyses in which all bays are assumed to have equal strength. In an effort to counteract the weakening influences of bulkheads, the David Taylor Model Basin developed a procedure[1] for obtaining an optimum design by which all frames deflect the same amount at failure and no bay is weakened by the influence of the bulkheads. The method used to obtain this result was to adjust the distance between the bulkhead and the first frame and the size of this first frame. To validate the adequacy of this design procedure, a series of model tests was made. The results of the tests were reported in Reference 2.

In Reference 1 it was also suggested that other design methods might be possible if at least two of the dimensions of the stiffened cylinders could be adjusted. Therefore, two identical models were made in which the thickness of plating and length of thickened plating away from the bulkhead were adjusted. The procedure used for designing these models is discussed in Appendix A.

The fabrication and instrumentation of these two models and the results of the tests conducted upon them are described in this report. In addition, this method of thickening plating at the bulkheads is compared with that of adjusting the spacing and size of the end frames.

DESCRIPTION OF MODELS

Models EB-13 and EB-14 were designed to study the effect of increasing the shell thickness in the vicinity of the end bulkhead rather than varying the length of the end bay and the size of the first frame. These two identical models were machined from a forged

---

[1]References are listed on page 16.

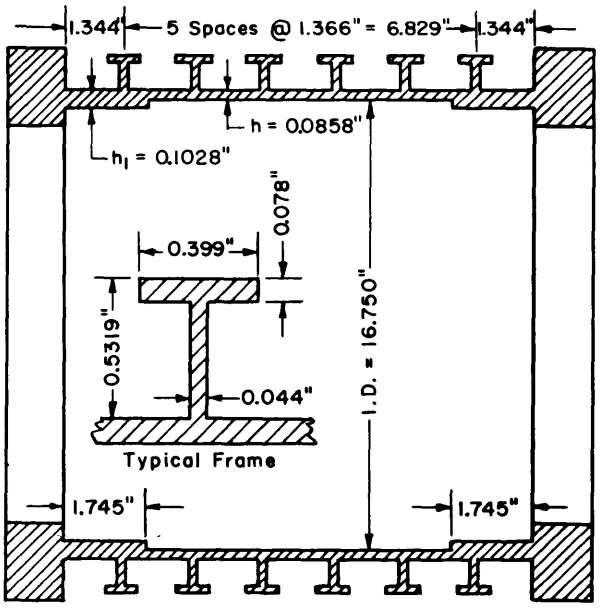

Figure 1 – Schematic Diagram of Models EB-13 and EB-14

steel gun barrel liner in order to substantiate the collapse pressure of the selected design. Yield strength of the material was determined from specimens which were taken from the liner and evaluated as described in Reference 2. The average value of the compressive yield strength for both models was 68,000 psi. A Young's modulus of 30,000,000 psi and a Poisson's ratio of 0.3 were assumed.

Model geometries and details of construction are available in Figure 1. Basically, all frames and frame spacings were machined to the dimensions specified for the typical sections of the models reported in Reference 2; in addition, the shell was thickened for a specified distance from each end bulkhead.

Measurements taken in the laboratory prior to instrumentation and testing of each model showed a maximum deviation of 1.5 percent for thicknesses and 0.5 percent for other dimensions shown in Figure 1.

INSTRUMENTATION AND TEST PROCEDURES

Each model was instrumented on the interior and exterior surfaces with electrical resistance-type strain gages to obtain an indication of its behavior under load. On both models, gages were installed on two generators, 160 deg apart. Each generator was rather extensively instrumented on the centerlines of bays and frames as shown schematically in Table 1. The gage locations were selected to provide strain distributions along the length of the models which could be compared with the strains calculated by the theory.

After each model had been instrumented, all external gages were subjected to a pressure of 1000 psi while the model was free flooded to determine any sensitivity of the gages to pressure. It was assumed that the strain gage was satisfactory when the difference in the strain measurements taken at no load and at 1000 psi was less than 50 μin/in. Those gages measuring strains in excess of 50 μin/in. were replaced.

Each model was tested in the Model Basin 20-in. diameter, 3000-psi pressure tank. Since the volume of the model was small compared with that of the tank, the volume of the tank was reduced to minimize the energy released at failure and, hence, the damage to the models. The volume was reduced by placing a heavy steel cylinder in the bottom of the tank. Oil was used as the pressure medium.

At least two loading runs were conducted for each model in an effort to minimize the nonlinearity of strains and thus ensure a more precise determination of strain-sensitivity

TABLE 1

Gage Locations on Instrumented Generators of Models

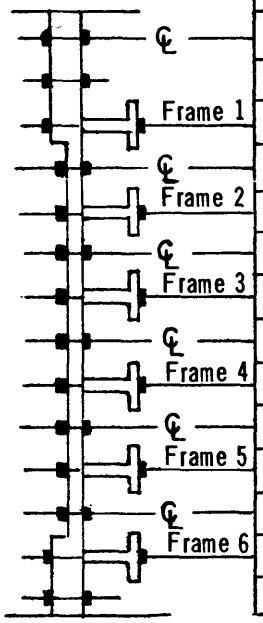

Gage Position	Ratios of Distances from Nearest Frame to Frame Spacing			
	EB-13		EB-14	
	0°	160°	0°	160°
1	0.50	0.50		
2			0.35	
3	0	0	0	
4	0.50	0.50	0.50	
5	0	0	0	0
6	0.50	0.50	0.50	0.50
7	0	0	0	0
8	0.50	0.50	0.50	0.50
9	0		0	0
10	0.50		0.50	0.50
11	0		0	0
12	0.50		0.50	
13	0		0	
14			0.35	

factors (the slopes of pressure-strain plots). Pressure increments were measured by means of a 1000-psi Bourdon-tube gage graduated in 5-psi increments. Strains were recorded at selected pressures with either Baldwin strain indicators or Gilmore automatic strain recorders.

TEST RESULTS

Both models failed at 990 psi by axisymmetric yielding, as evidenced by corrugation of the shell between frames. For both models, deformation occurred very slowly with practically no noise, and the accompanying drop in pressure stabilized at approximately 600 psi. Failures were identical in form and occurred in the third bay from a bulkhead where they extended for about 270 deg around the circumference of the model. Figure 2 shows the location and extent of damage typical of both models.

Strain-sensitivity factors in microinches per inch per psi of pressure are given in Table 2. The circumferential strain-sensitivity factors are averaged values for the interior and exterior surfaces. The value given for each location is the average of the values at similar locations on two generators. Typical pressure-strain curves from which these sensitivity factors were obtained are presented in Figure 3. These curves indicate that yielding occurred near the theoretical yield pressure which is about 90 percent of the collapse pressure. Hence residual stresses present in the model after fabrication were negligible.

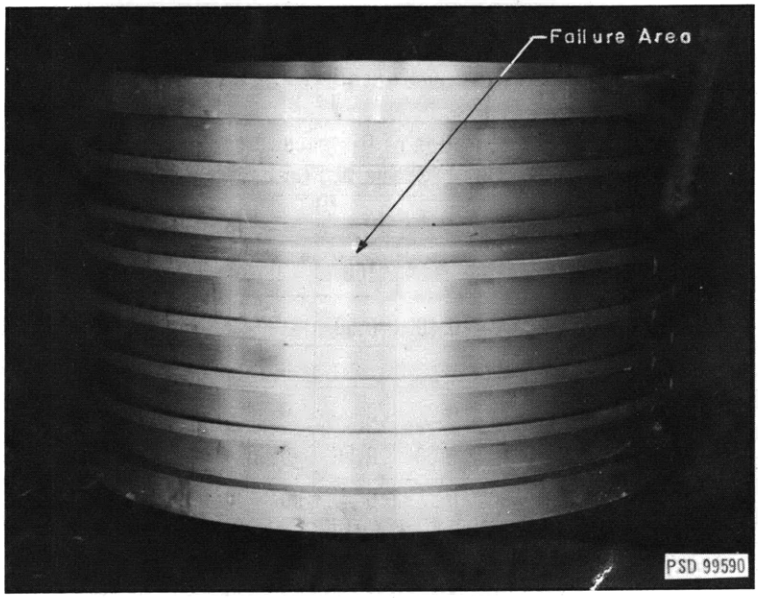

Figure 2 – Model EB-13 after Collapse

TABLE 2

Experimental Strain-Sensitivity Factors

General Location	Distance (x/L) in Terms of Bay Length	Strain Sensitivity Factors, μ in./in./psi					
		Circumferential*		Longitudinal Exterior		Longitudinal Interior	
		EB-13	EB-14	EB-13	EB-14	EB-13	EB-14
Upper End Bay	0.50 0.65	−1.15	−1.18	−1.32	−1.40	−0.30	−0.20
First Frame	1.00	−1.51	−1.54			−0.84	−0.72
Bay	0.50	−1.98	−1.88	−1.33	−1.26	−0.31	−0.28
Second Frame	1.00	−1.73	−1.63			−1.60	−1.61
Bay	0.50	−1.96	−1.86	−1.28	−1.23	−0.33	−0.38
Third Frame	1.00	−1.70	−1.67			−1.62	−1.68
Bay	0.50	−1.96	−1.90	−1.32	−1.28	−0.32	−0.37
Fourth Frame	1.00	−1.78	−1.66			out	−1.67
Bay	0.50	−1.93	−1.86	out	−1.26	−0.24	−0.37
Fifth Frame	1.00	−1.76	−1.68			out	−1.58
Bay	0.50	−2.01	−1.77	−1.32	−1.28	−0.36	−0.38
Sixth Frame	1.00	−1.63	−1.63			out	−0.71
Lower End Bay	0.35		−1.28		−1.38		−0.18

*Circumferential strain-sensitivity factors are averaged values for external and internal gages and for similar locations on two generators.

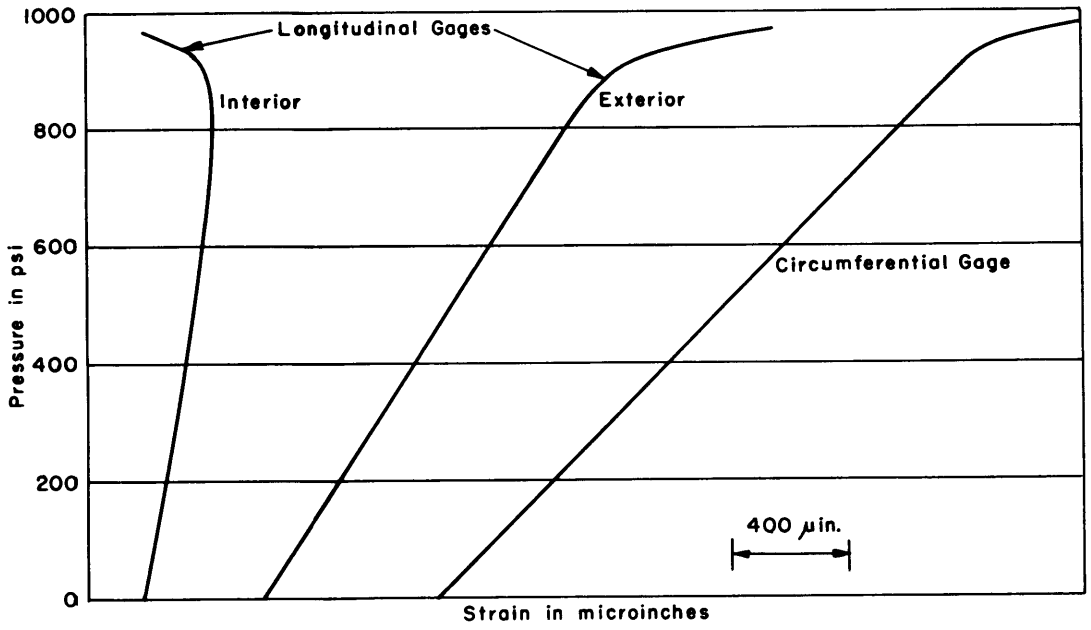

Figure 3 – Typical Pressure-Strain Plots of Midbay Gages for Models EB-13 and EB-14

TABLE 3

Summary of Experimental and Theoretical Collapse Pressures

Model	Yield Strength of Shell Material psi	Experimental Collapse Pressure, psi		Case	Averaged Experimental Collapse Pressure psi	Averaged Experimental Collapse Pressure / Maximum Averaged Experimental Collapse Pressure = Col 6 / 987	Failure Bay from Bulkhead	Minimum Theoretical Plastic Hinge Pressure in Bay of Failure		Theoretical Plastic Hinge Pressure in Bay of Failure Adjusted by Eq.[1]	
		Actual	Adjusted to σ_y = 67,000 psi					psi	Experimental / Theoretical = Col 6 / Col 9	psi	Experimental / Theoretical = Col 6 / Col 11
1	2	3	4	5	6	7	8	9	10	11	12
EB-5	68,800	960	934	I	942	0.954	2	930	1.013	947	0.995
EB-6	67,000	950	950								
EB-3	65,800	921	938	II	938.5	0.951	2	867	1.082	941	0.997
EB-4	66,000	925	939								
EB-7	68,700	955	932	III	936	0.948	1	901	1.039	921	1.016
EB-8	68,800	965	940								
EB-1	66,400	975	984	IV	981.5	0.994	1	905	1.085	934	1.051
EB-2	66,800	975	979								
EB-9	66,700	950	953	V	950.5	0.963	2	949	1.002	962	0.988
EB-10	67,200	952	948				3	967	0.983	965	0.985
EB-11	64,800	950	982	VI	987	1.000	1	922	1.070	953	1.036
EB-12	64,800	960	992				3	963	1.025	965	1.023
EB-13	67,800	988	977	VII	974.5	0.987	3	963	1.012	965	1.010
EB-14	68,200	990	972								

DISCUSSION OF RESULTS

Table 3 contains the yield strength of the shell material, Column 2, the experimental collapse pressure, Column 3, and the failure area, Column 8, for each of the models. Similar information is given for Models EB-1 through EB-12, previously reported in Reference 2, to facilitate evaluation of the models.

Since the yield strengths of the models varied significantly, as shown by the second column of Table 3, the collapse pressures of the different models cannot be compared directly with one another until they have been adjusted to a common yield strength. The yield strength selected for this adjustment was 67,000 psi, the average of all the models in the series. The collapse pressures were adjusted by the ratio of the average yield strength to the actual yield strength and are given in Column 4 of Table 3.

The adjusted experimental collapse pressures have been averaged for identical models in Column 6. The ratios of the averaged pressures to the maximum averaged pressure are given in Column 7. Comparison of these ratios shows that Case VII models are four percent stronger than similar models with uniform shell thickness and the end bays two-thirds the length of the others.

Adjusted collapse pressures of Models EB-13 and EB-14 differed by 0.5 percent. The maximum difference between "identical" models of the series was 1.7 percent (Case I), and the minimum difference was 0.1 percent (Case II). The average of these differences for the entire series was 0.7 percent. This variation in adjusted collapse pressures is an indication of the experimental error of the series of 14 model tests.

As a further check on the validity of the test results, the minimum plastic hinge pressure[3] which occurred near, but not necessarily at, the middle of the bay was computed for the bay in which failure occurred in each model, using the elastic stresses computed by the end-bay theory[1] at the actual collapse pressure. Also, an adjusted plastic-hinge pressure was computed because there was a considerable variation in the stress patterns in the bays of failure. The adjusted plastic-hinge pressure, p_{adj}, for a bay was computed from the equation

$$\frac{2}{p_{adj}} = \frac{1}{p_1}\left(1-\frac{a}{l}\right) + \frac{1}{p_{min}} + \frac{1}{p_2}\left(\frac{a}{l}\right) \qquad [1]$$

where p_1 and p_2 are the pressures at which plastic hinges form in the shell adjacent to the frames, neglecting shearing stresses,

p_{min} is the lowest pressure at which a hinge will form in the interior of the bay near, but not necessarily at, the midpoint,

a is the distance of the interior hinge from the first frame of that bay, and

l is the clear distance between frames.

All these pressures are based on the assumption that internal forces remain proportional to loads in the yield range. Equation [1] is based on an analogy to a fixed-end beam of constant

section but nonunifofmly loaded and is developed in Appendix B. The plastic-hinge pressures are presented in Table 3. For this series of models the adjusted plastic-hinge pressures agree more closely with the experimental collapse pressure than the midbay plastic-hinge pressure. The collapse pressure for an end bay exceeds the adjusted plastic-hinge pressure, while collapse in any other bay agrees reasonably well with the adjusted plastic-hinge pressure. The adjusted plastic-hinge pressures indicate that the initial collapse for Case-V models probably occurred in Bay 2 instead of Bay 3 as reported in Reference 2.

In Figure 4, strains measured for Models EB-13 and EB-14 are compared with strain curves derived from the theory of Reference 1. Two theoretical curves are shown: one for the elastic strain sensitivities before yielding occurs at the bulkheads (obtained for a pressure of 200 psi) and the other for strain sensitivities obtained after yielding at the bulkheads and near collapse pressure (obtained for a pressure of 900 psi). The experimental strains plotted in Figure 4 were obtained by averaging sensitivities for similar locations on EB-13 and EB-14. Experimental strains are, in general, slightly less than the theoretical strains in both the elastic and yield ranges as illustrated by Figure 4.

The most probable source of error in measuring strains is poor bonding of the gage to the model, which would always result in low strain readings. Another possible cause of discrepancy between theoretical and experimental strains is the use of an incorrect Young's modulus. For these tests, however, the value of Young's modulus required to attain good agreement of the strains is abnormally high.

Both theoretical and experimental strains indicate that the effect of the bulkhead is not appreciable in the third bay of either of the two models, EB-13 and EB-14. This was also observed in the earlier tests described in Reference 2. Therefore, it seems reasonable to expect that any design of end bays which shifts failure as much as two bays away from a bulkhead is a satisfactory design.

The design used for Case-VII models requires the addition of somewhat more weight than that used for Case-VI models. This additional weight amounts to 1 percent of the weight of a Case-VI compartment two diameters long. The theoretical longitudinal elastic strain-sensitivity factors at the bulkhead for Case-VII models were 4.68 μin/psi in compression on the inside and 2.20 μin/psi in tension on the outside compared with 5.61 μin/psi in compression on the inside and 2.63 μin/psi in tension on the outside for Case-VI models. This reduction in maximum stress should provide an increase in fatigue life. Also, there was no evidence, either experimental or theoretical, of failure in the first or second bays of the Case-VII models. Another advantage of this design is that no alteration to frame spacing is required.

Attention is further directed to the fact that the test results do not indicate the adequacy of this design for a cylinder containing residual welding and rolling stresses. It is believed, however, that the strength of this design will be less affected at the ends by residual stresses than the designs of Reference 2 because of the lower stress level in the end bays.

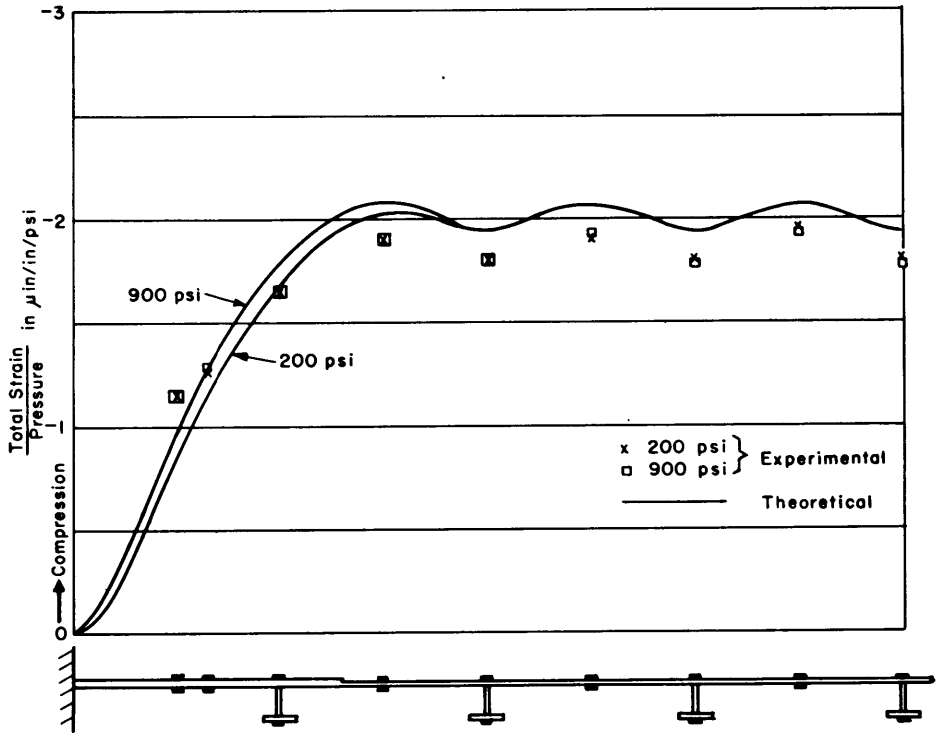

Figure 4a – Circumferential Strains, Exterior and Interior Surfaces

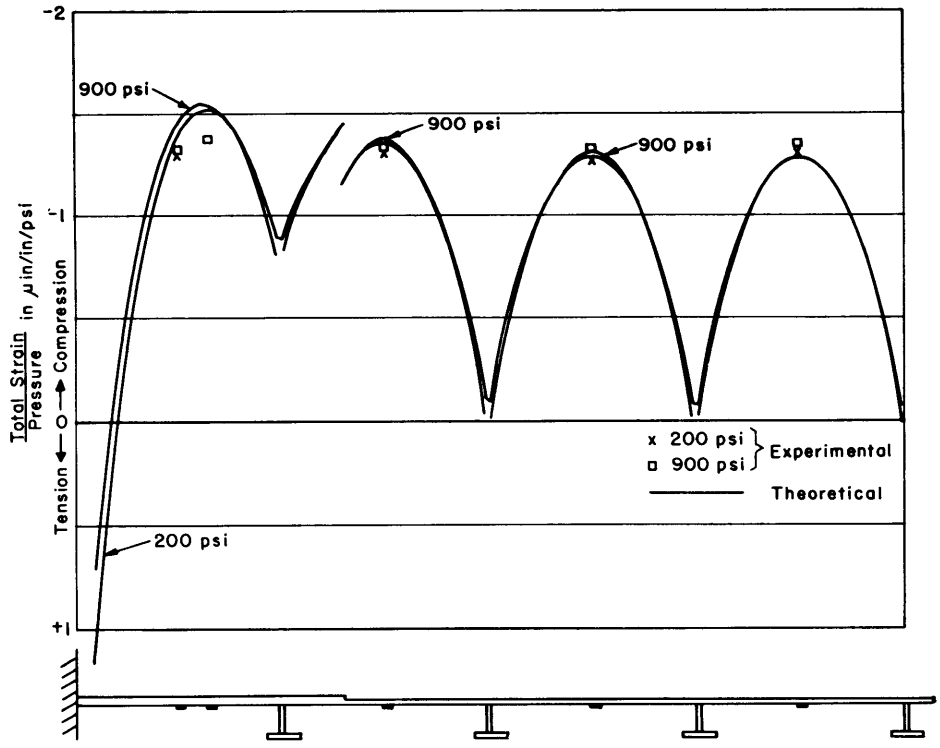

Figure 4b – Longitudinal Strains, Exterior Surface

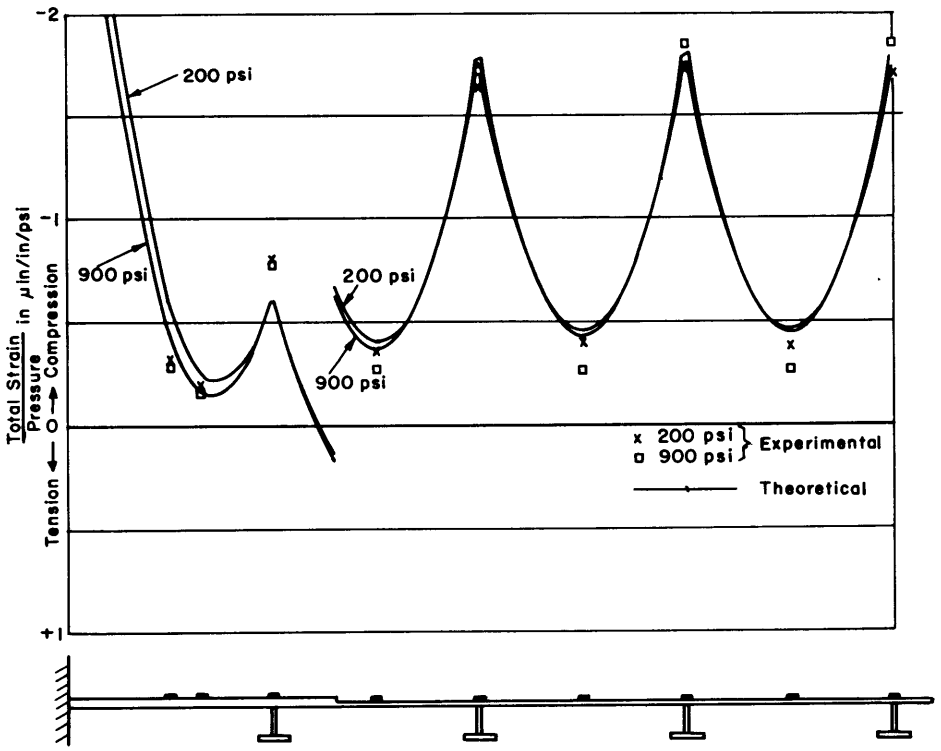

Figure 4c – Longitudinal Strains, Interior Surface

Figure 4 – Comparison of Theoretical Strain Distributions with Experimental Strain Distributions for Models EB-13 and EB-14

CONCLUSIONS

The experimental and theoretical results for the machined ring-stiffened cylinders of the geometry tested indicate that:

1. The effect of end conditions on the strength of ring-stiffened cylinders can be practically eliminated by proper design using a thicker shell near the ends, and the failure can be shifted away from the ends.

2. The design presented in this report may be as much as 4 percent stronger than arbitrary end designs, although possibly somewhat weaker than the best design of Reference 2.

3. The maximum longitudinal stress, which occurred at the bulkhead, was reduced to 84 percent of that in the optimum models of Reference 2.

4. The additional weight required for this design is slightly more than that required for Case-VI models, the optimum design discussed in Reference 2.

APPENDIX A

DESIGN OF ENDS OF MODEL

In Reference 1 it was suggested that equal strength bays of a ring-stiffened cylinder loaded by uniform external pressure could be designed if any two model parameters near the bulkhead could be adjusted so that the deflection, and hence the stresses, for a given pressure of all subsequent parts of the cylinder would be identical to those of a long cylinder with equally spaced frames. Models EB-13 and EB-14 were built to check a design in which the thickness and width of the shell plating adjacent to the bulkheads were increased.

In the following discussion it is assumed that the thicker plating will end in the second bay. This is usually true; however, it is not necessary for the solution.

In Reference 1 a procedure is developed for a ring-stiffened circular cylinder under uniform pressure loading whereby a matrix

$$|B|_{0,1} = \begin{vmatrix} y \\ y'/\alpha \\ y''/2\alpha^2 \\ y'''/2\alpha^3 \\ y_u \end{vmatrix}_{0,1} \qquad [2]$$

can be transformed into any other matrix

$$|B|_{x,m} = \begin{vmatrix} y \\ y'/\alpha \\ y''/2\alpha^2 \\ y'''/2\alpha^3 \\ y_u \end{vmatrix}_{x,m} \qquad [3]*$$

in which y is the radial deflection of the shell, primes denote derivatives with respect to x, the distance along a generator, and $\alpha = \sqrt[4]{3(1-\nu^2)}/\sqrt{Rh}$ where R is the mean shell radius and h is the shell thickness. The deflection of an unstiffened shell is

*This is a generalization of Equation [20] of Reference 1.

$$y_u = \frac{pR^2}{Eh}\left(1-\frac{\nu}{2}\right)$$

where p is external pressure,

E is Young's modulus, and

ν is Poisson's ratio.

The subscript x,m indicates that the matrix is evaluated at a distance x from a frame in the mth bay from the starting point. This transformation is accomplished by premultiplying $|B|_{0,1}$ by a sequence of 5 x 5 matrices, first by $|S|_{l,i}$, then by $|F|_{i,\ i+1}$, where i takes on all integral values from 1 to $m-1$, and finally by $|S|_{x,m}$. The matrix $|S|_{l,i}$ transforms the matrix $|B|_{o,i}$ to $|B|_{l,i}$ and is called a bay matrix. $|F|_{i,\ i+1}$ transforms $|B|_{l,i}$ to $|B|_{o,\ i+1}$ and is called a frame matrix.

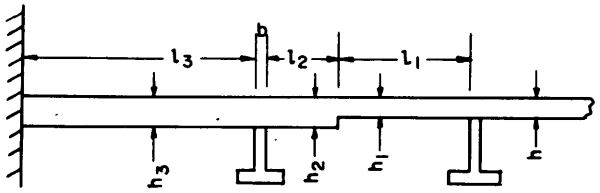

Figure 5 – Nomenclature for Design of Models EB-13 and EB-14

Figure 5 is a section along a generator of Models EB-13 and EB-14 showing the nomenclature to be used. Where there is a change in shell thickness as exists in these models, an $|F|$ matrix is required to relate the $|B|$ matrices on both sides of this change. This, in effect, divides this bay into two bays. Thus $|B|_{l_3,3}$ at the bulkhead is expressed in terms of $|B|_{o,1}$ by the equation:

$$|B|_{l_3,3} = |S|_{l_3,3} \times |F|_{2,3} \times |S|_{l_2,2} \times |F|_{1,2} \times |S|_{l_1,1} \times |B|_{0,1} \qquad [4]$$

The $|S|$ matrices are defined by Equation [11] of Reference 1, while $|F|_{2,3}$ is defined by Equation [17] of Reference 1. Since the shell radii and thicknesses are the same for Bays 2 and 3, the equation for $|F|_{2,3}$ can be simplified to the following:

$$|F|_{2,3} = \begin{vmatrix} 1 & b\alpha & 0 & 0 & 0 \\ 0 & 1 & 0 & 0 & 0 \\ -(b\alpha)^2 \dfrac{A_F + bh}{bh} & (b\alpha)^3 \left[\dfrac{2I_F + \dfrac{b^3 h}{6}}{b^3 h} - \dfrac{A_F + bh}{2bh} \right] & 1 & b\alpha & (b\alpha)^2 \\ -2(b\alpha) \dfrac{A_F + bh}{bh} & -(b\alpha)^2 \dfrac{A_F + bh}{bh} & 0 & 1 & 2b\alpha \\ 0 & 0 & 0 & 0 & 1 \end{vmatrix} \quad [5]$$

where A_F and I_F are the effective area and moment of inertia of a frame against twist, respectively, and b is its faying width. $|F|_{1,2}$ is obtained from equations of equilibrium and continuity at the change in shell thickness which are:

$$y_2(0) = y_1(l_1) \quad [6a]$$

$$y_2'(0) = y_1'(l_1) \quad [6b]$$

$$R_2 M_2(0) = R_1 M_1(l_1) + (p/6)(R_1^3 - R_2^3) \quad [6c]$$

$$R_2 V_2(0) = R_1 V_1(l_1) \quad [6d]$$

where M and V are longitudinal bending moment and shear force per unit circumference of the shell. Solution of Equations [6] for y_2, y_2'/α_2; $y_2''/2\alpha_2^2$; $y_2'''/2\alpha_2^3$, and y_{u2} at $x = 0$ in terms of y_1, y_1'/α_1, $y_1''/2\alpha_1^2$, $y_1'''/2\alpha_1^3$, and y_{u1} at $x = l_1$ shows that:

$$|F|_{1,2} = \begin{vmatrix} 1 & 0 & 0 & 0 & 0 \\ 0 & \dfrac{\alpha_1}{\alpha_2} & 0 & 0 & 0 \\ 0 & 0 & \left(\dfrac{h_1}{h_2}\right)^2 & 0 & \dfrac{2}{(2-\nu)}(R_2\alpha_2)^2 \left(\dfrac{R_2}{R_1} - 1\right)\left(\dfrac{h_1}{h_2}\right) \\ 0 & 0 & 0 & \left(\dfrac{\alpha_1}{\alpha_2}\right)\left(\dfrac{h_1}{h_2}\right)^2 & 0 \\ 0 & 0 & 0 & 0 & \left(\dfrac{R_2}{R_1}\right)^2 \left(\dfrac{h_1}{h_2}\right) \end{vmatrix} \quad [7]$$

The procedure is to compute the elements of $|B|_{o,1}$ by the analysis of Salerno and Pulos[4] for equally spaced identical frames. Two linear equations defining the elements of $|B|_{l_3,3}$ are obtained from the physical properties of the bulkhead. Thus Equation [4] represents four algebraic equations defining two unknown elements of $|B|_{l_3,3}$ and the thickness and width of plating adjacent to the bulkhead. These four equations are easily reduced to two by elimination of the two unknown elements of $|B|_{l_3,3}$. The two remaining equations for the thickness and width of plating adjacent to the bulkhead were solved by Newton's method which is outlined in the Appendix of Reference 5. The solution was programmed for the IBM 704 since it is very long and tedious.

APPENDIX B

LIMIT LOAD OF A FIXED END BEAM

The limit load of a beam composed of elastic, perfectly plastic material is reached when hinges are formed at the supports and a third hinge is formed between the supports at some distance, a, from the left end. The beam to be considered here (Figure 6) is of constant cross section with a length l. It is loaded by $q \cdot f(x)$ where f is a function of x only, the distance from the left end of the beam, and q is the magnitude of load. The beam is supported by shear forces and moments V_1 and M_1 at $x = 0$ and V_2 and M_2 at $x = l$. The magnitude of the internal moment at $x = a$ is M_3.

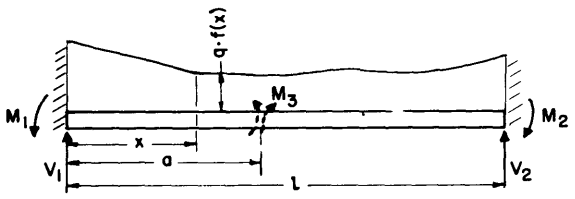

Figure 6 – Nomenclature for Fixed End Beam under Nonuniform Load

The force and moment equilibrium equations are:

$$V_1 + V_2 = \int_o^l qf(x)\,dx \qquad [8]$$

$$M_1 + M_3 = V_1 a - \int_o^a q(fx)\,(a - x)\,dx \qquad [9]$$

$$M_2 + M_3 = V_2\,(l-a) - \int_o^l qf(x)\,(x-a)\,dx \qquad [10]$$

Eliminating the shear forces from Equations [8], [9], and [10] gives

$$M_1\left(1-\frac{a}{l}\right) + M_2\left(\frac{a}{l}\right) + M_3 = q\left[\frac{a}{l}\int_o^l (l-x)\,f dx + \int_o^a x \cdot f dx\right] = \gamma q \qquad [11]$$

At the limit load q_L:

$$M_1 = M_2 = M_3 = M_L \qquad [12]$$

and, therefore,

$$\gamma = \frac{2M_L}{q_L} \qquad [13]$$

where M_L is the limit moment for a cross section of the beam. Now let

$$M_1 = \frac{q}{q_1} M_L$$

$$M_2 = \frac{q}{q_2} M_L \qquad [14]$$

$$M_3 = \frac{q}{q_3} M_L$$

Then q_1, q_2, and q_3 are the loads which would produce hinges at Locations 1, 2, and 3, respectively, if the internal forces remained proportional to the load even after yielding. Substituting Equations [13] and [14] into [11] results in:

$$\frac{2}{q_L} = \frac{1}{q_1}\left(1-\frac{a}{l}\right) + \frac{1}{q_2}\left(\frac{a}{l}\right) + \frac{1}{q_3} \qquad [15]$$

The value of a which gives the minimum q_L is not necessarily that which gives the minimum q_3. However, it is usually near that, and the values of q_L differ only slightly for the cases of interest in this report.

Equation [15] gives the limit load in terms of the "plastic hinge loads" for a beam. For a cylinder q is replaced by p and

$$f(x) = 1 - \frac{\nu}{2} - \frac{Eh}{pR^2}\, y(x) \qquad [16]$$

expresses the difference between a unit radial pressure and the radial shell reaction for a unit pressure. Because of the biaxial state of stress, M_L is not a constant throughout the bay. However, this method is proposed because it takes into account the stress distribution in the bay, and, more important, it is found to agree well with experimental collapse in both symmetric and nonsymmetric bays.

REFERENCES

1. Short, R.D. and Bart, R., "The Effects of End Conditions on the Stresses in Stiffened Cylindrical Shells," David Taylor Model Basin Report 1065 (Jun 1959).

2. Keefe, R.F. and Overby, J.A., "An Experimental Investigation of Effect of End Conditions on Strength of Stiffened Cylindrical Shells," David Taylor Model Basin Report 1326 (Dec 1959).

3. Lunchick, M.E., "Yield Failure of Stiffened Cylinders under Hydrostatic Pressure," David Taylor Model Basin Report 1291 (Jan 1959).

4. Salerno, V.L. and Pulos, J.G., "Stress Distribution in a Circular Cylindrical Shell under Hydrostatic Pressure Supported by Equally Spaced Circular Ring Frames," Polytechnic Institute of Brooklyn Aeronautical Laboratory Report No. 171-A, (Jun 1951).

5. Brock, Joseph S., "Analytical Determination of the Stresses around Square Holes with Rounded Corners," David Taylor Model Basin Report 1149 (Nov 1959).

INITIAL DISTRIBUTION

Copies

14 CHBUSHIPS
- 3 Tech Info Sec (Code 335)
- 1 Tech Asst (Code 106)
- 1 Lab Mgt (320)
- 1 Prelim Des Br (Code 420)
- 1 Prelim Des Sec (Code 421)
- 1 Ship Protec (Code 423)
- 1 Hull Des Br (Code 440)
- 2 Sci & Res Sec (Code 442)
- 1 Struc (Code 443)
- 1 Submarine Br (Code 525)
- 1 Hull Arr, Struc, & Preserv Br (Code 633)

2 CHONR
- 1 Struc Mech Br (Code 439)
- 1 Undersea Programs (Code 466)

1 CNO
Submarine Readiness Warfare (Op 311)

1 CDR, USNOL, White Oak

1 DIR, USNRL
Attn: TID (Code 2020)

2 NAVSHIPYD PTSMH

2 NAVSHIPYD MARE

2 NAVSHIPYD CHASN

1 DATMOBAS, UERD (Code 780), Portsmouth

10 CDR, ASTIA

1 SUPSHIP, Groton

1 EB Div, Gen Dyn Corp

1 SUPSHIP, NNS

1 NNS SB & DD Co

1 SUPSHIP, Pascagoula

1 Ingalls SB Corp

1 SUPSHIP, Camden

1 New York SB Corp

1 Dir of Def R & E
Attn: Tech Lib

1 CO, USNROTC & NAVADMINU MIT

1 O in C, PGSCOL, Webb

David Taylor Model Basin. Report 1513.
A METHOD FOR ELIMINATING THE EFFECT OF END CONDITIONS ON THE STRENGTH OF STIFFENED CYLINDRICAL SHELLS, by Robert F. Keefe and Robert D. Short, Jr. Sep 1961. iii, 19p. illus., photos., graphs, tables, refs. UNCLASSIFIED

A pair of stiffened cylinders was subjected to external hydrostatic pressure to establish the adequacy of a design procedure for eliminating the effect of end conditions on strength. The cylinders were machined from a thick tube and were identical to those described in TMB Report 1326 except for the size and spacing of the frames and the thickness of the shell at the ends. The cylinders failed by axisymmetric shell yielding in the second full-length bay at identical collapse pressures. Test results indicated that, with these end conditions, the collapse pressure could be increased by 4 percent over that for a similar model in which the first bay length was two thirds of the length of the others, and failure could be shifted away from the ends of the cylinder.

1. Cylindrical shells (Stiffened)--Stresses--Measurement
2. Cylindrical shells (Stiffened)--Strength--Test results
I. Keefe, Robert F.
II. Short, Robert D.
III. S-F013 03 02